Genome-wide changes in genetic diversity in a *Myotis lucifugus* population affected by white-nose syndrome

Lilley TM [1,2], Wilson IW [1], Field KA [3], Reeder DA [3], Turner G [4], Kurta A [5], Blomberg AS [6], Hoff S [7], Herzog C [7], Paterson S [1].

[1]Institute of Integrative Biology, University of Liverpool, United Kingdom. [2]Finnish Museum of Natural History, University of Helsinki, Finland. [3]Biology Department, Bucknell University, 1 Dent Drive, Lewisburg, PA 12837, USA. [4]Pennsylvania Game Commission, Harrisburg, PA, USA. [5]Department of Biology, Eastern Michigan University, Ypsilanti, MI, USA. [6]Department of Biology, University of Turku, Finland. [7]Wildlife Diversity Unit, State Department of Environmental Conservation, Albany, NY, USA.

Corresponding author: tmlill@liverpool.ac.uk

Abstract

Novel pathogens can cause massive declines in populations, but seldom lead to extirpation of hosts. Rather, disease can act as a selective pressure on survivors, driving the evolution of resistance or tolerance. Bat white-nose syndrome (WNS) is a rapidly spreading wildlife disease in North America. The fungus causing the disease invades skin tissues of hibernating bats, resulting in disruption of hibernation behavior, premature energy depletion, and subsequent death. We use whole-genome sequencing to investigate changes in allele frequencies within a population of *Myotis lucifugus* in eastern North America, to scan for genetic resistance to WNS. Our results show low F_{ST} values within the population across time, i.e. prior to WNS (Pre-WNS) compared to population that has survived WNS (Post-WNS). However, when dividing the population with an arbitrary geographical cut-off between the states of Pennsylvania and New York, a sharp increase in values on scaffold GL429776 is evident in the Post-WNS samples. The genes present in the diverged area cannot be directly associated with selection caused by WNS based on previous literature. Thus, we conclude that WNS has not subjected *M. lucifugus* to selective pressure but may have allowed the rise of a selection for alleles in Pennsylvania through decreased gene flow within the population. Therefore, the existence of remnant sub-populations in the aftermath of WNS is likely due to other factors in bat life history besides genetic adaption.

Keywords: Opportunistic pathogen, white-nose syndrome, Selective pressure, Genetic resistance.

1. Introduction

The emergence and spread of multiple infectious wildlife diseases during recent decades has had devastating consequences for biodiversity (Daszak et al., 2000; Smith et al., 2006). Unfortunately, for many taxa, anthropogenic activities and climate change appear to be the main causes of exposure to sources of infection (Gallana et al., 2013; Tompkins et al., 2015). With shifting pathogen ranges, disease-related declines in naïve wildlife often threaten the persistence of populations. Examples include chytridiomycosis, which has wiped out populations of amphibians globally (Daszak et al., 1999; Lips et al., 2006), and avian malaria, which caused the sharp decline of island populations of birds (van Riper et al., 1986). More recently, white-nose syndrome (WNS) has been described as one of the most rapidly spreading wildlife diseases ever recorded (Blehert et al., 2009; Frick et al., 2010). Since the discovery of WNS in North America in 2006, ten species of bats have been diagnosed with the disease in 33 U.S. states and 7 Canadian provinces (www.whitenosesyndrome.org, 2019). Genetic evidence suggests that *Pseudigymnoascus destructans*, the causative agent of WNS, was introduced to North America from Europe (Campana et al., 2017; Lorch et al., 2013; Minnis and Lindner, 2013; Ren et al., 2012; Wibbelt et al., 2010), where affected species do not experience associated mortality (Harazim et al., 2018; Puechmaille et al., 2011; Warnecke et al., 2012; Wibbelt et al., 2013; Zukal et al., 2016).

When a disease enters a naïve host population, the initial wave of infection often causes epizootics that result in mass mortality, which may extirpate local host populations or even cause species extinction (Daszak et al., 1999; De Castro and Bolker, 2005; Frick et al., 2010). However, extinctions due to a disease appear to occur seldomly, and a disease can act as a

56 selective pressure on survivors, driving the evolution of tolerance or resistance, which may
57 transform a disease from being epizootic to being enzootic (Boots et al., 2009; Karlsson et al.,
58 2014; Robinson et al., 2012). This may occur through rapid changes in the distribution of
59 genetic variants associated with disease susceptibility over short timescales (Gallana et al.,
60 2013). These powerful selective pressures pathogens exert on naïve host populations (Sironi
61 et al., 2015) and genetic signatures of infection-related selective sweeps may be detectable for
62 generations (Deschamps et al., 2016; Di Gaspero et al., 2012; Groot et al., 2002). Detection of
63 selective sweeps on particular genes or gene families can confirm or exclude potential
64 mechanisms of host susceptibility or pathogen virulence (Campbell and Tishkoff, 2008).
65 Rapid, extreme bottlenecks (such as those caused by panzootic events), meanwhile, are
66 associated with a more stochastic loss of alleles, which does not necessarily indicate selection
67 (Luikart et al., 1998). Much of the research on disease-induced selection has focused on the
68 major histocompatibility complex (MHC), and indeed, diseases can drive the evolution and
69 maintenance of MHC diversity in natural populations (Davy et al., 2017a; Jeffery and
70 Bangham, 2000; Paterson et al., 1998; Spurgin and Richardson, 2010; Teacher Amber G. F. et
71 al., 2009; Zeisset and Beebee, 2014). However, factors not directly associated with interactions
72 between host and pathogen, such as environmental conditions and competition with other
73 species, can have a considerable influence on the manifestation of a disease (Scholthof, 2007).

74 The psychrophilic (cold-growing) fungus *P. destructans*, (Lorch et al., 2011; Minnis and
75 Lindner, 2013; Warnecke et al., 2008) acts as an opportunistic pathogen of bats, invading the
76 skin tissues of hibernating hosts (Cryan et al., 2010; Meteyer et al., 2012). Susceptible species,
77 such as *M. lucifugus* and *M. septentrionalis*, have shown population declines greater than 90%
78 in affected hibernacula (Frick et al., 2015). The infection disrupts the hibernation behaviour of

79 the bats and leads to more frequent arousals from torpor, evaporative water loss, premature
80 energy depletion, and death of susceptible individuals due to emaciation (McGuire et al., 2017;
81 Reeder et al., 2012; Verant et al., 2014; Warnecke et al., 2013; Willis et al., 2011). Naïve
82 infected *M. lucifugus* upregulate genes involved in immune pathways during hibernation (Davy
83 et al., 2017b; Field et al., 2015, 2018; Lilley et al., 2017). These responses are weak during
84 torpor but are robust after arousal, supporting the hypothesis that periodic arousals are
85 necessary to initiate immune responses to pathogens or to augment responses that occur at low
86 levels during torpor (Field et al., 2018; Luis and Hudson, 2006). Therefore, increased arousals
87 may be attempts by the host to fight off the pathogen, in addition to quenching thirst, expelling
88 waste and possibly foraging (Bernard and McCracken, 2017; Willis et al., 2011) and
89 supplementing electrolytes (Cryan et al., 2013). White-nose syndrome is a prime example of a
90 disease which is manifested when factors associated with the environment (i.e. temperature
91 and humidity of the hibernaculum), the host (and the host's response to infection) and the
92 pathogen correlate favourably (Scholthof, 2007). Therefore bat species, and populations within
93 species, are affected differently according to hibernation behaviour and prevailing micro-
94 climate conditions in available hibernacula (Grieneisen et al., 2015; Johnson et al., 2014;
95 Langwig et al., 2015). As such, with a wildlife disease dependent on outside host interactions,
96 such as WNS, loci not associated with MHC diversity or other immune response-associated
97 factors, such as the amount of body fat prior to hibernation (Cheng et al., 2019), may also affect
98 survival of species and populations. This highlights the importance of examining the genome
99 as a whole (Sparks et al., 2019).

100 The initial impacts of WNS on six species of hibernating bats in the northeastern and
101 midwestern USA vary from almost complete extirpation to arrested population growth (Turner

102 et al., 2011). After the initial decline caused by WNS in *M. lucifugus*, reports have surfaced
103 describing stabilisation at smaller sizes or even increases in numbers of individuals (Dobony
104 and Johnson, 2018; Frick et al., 2017; Langwig et al., 2015; Maslo et al., 2015). Models
105 parameterised with long-term data on fungal loads, infection intensity and counts of bats at
106 hibernacula have suggested development of either tolerance or resistance in these persisting
107 populations (Frick et al., 2017), which is supported by reports on infected bats not arousing
108 from torpor as frequently as during the acute phase of the zoonosis (Lilley et al., 2016). Since
109 WNS has inflicted massive population declines in some species, there is a possibility that
110 selection could occur for alleles conferring resistance or tolerance from the standing genetic
111 variation, which would confer to resistance or tolerance could occur. Indeed, Maslo and
112 Feffermann (2015) suggested the occurrence of evolutionary rescue occurring and Donaldson
113 et al. (2017) described changes in an immunome across *M. lucifugus* populations obtained
114 through a sequence capture method, which may be attributed to selection by WNS. A study
115 suggests the initially affected *M. lucifugus* population is beginning to show signs of resistance
116 to the pathogen (Langwig et al., 2017). However, the possible selective pressures WNS has
117 exerted on the population, which may not even be related to immune responses (e.g. Cheng et
118 al., 2019), are yet to be described at the whole-genome level using high-depth sequencing depth
119 (although see Gignoux-Wolfsohn et al., 2018).

120 Here, we utilise high-throughput whole-genome sequencing on the WNS-affected species *M.*
121 *lucifugus*, allowing us to look at entire genomes via single nucleotide polymorphisms (SNPs).
122 We compare genetic patterns (F_{ST} and heterozygosity) before and after the spread of WNS in
123 the eastern North American population to gain insight into whether the disease is causing
124 selection of major loci in surviving bats. We hypothesise that, due to the massive population

125 declines caused by WNS and the fact that the affected population is now beginning to stabilise
126 or slightly increase in size (Langwig et al., 2017), a soft selective sweep based on standing
127 genetic variation has resulted in differentiation in one or many regions of the genome (Messer
128 and Petrov, 2013). Adaptation could therefore be in the process of driving the evolutionary
129 rescue of a population, in which individuals resistant or tolerant to the disease survived a
130 bottleneck and passed these traits to their offspring (Carlson et al., 2014). Alternatively,
131 survival may be due to factors not related to selection for WNS-resistant alleles, such as
132 microbiome adaptation (Ange-Stark et al., 2019; Lemieux-Labonté et al., 2017) or stochasticity
133 in hibernation site microhabitat. This study provides a foundation for future work on genome-
134 wide effects of WNS in *M. lucifugus* and other affected species of bats.

135 2. Materials and methods

136 2.1. Ethics Statement

137 This study was carried out on bats from non-endangered species in strict accordance with
138 recommendations in the Guide for the Care and Use of Laboratory Animals of the National
139 Institutes of Health. All methods were approved by the Institutional Animal Care and Use
140 Committee at Bucknell University (protocol DMR-016). The bats were collected under
141 Pennsylvania Game Commission Special Use Permit #33085, and New York State Department
142 of Environmental Conservation Permit #427.

143 2.2. Sample collection and DNA extraction

144 We conducted whole-genome sequencing on a population of *M. lucifugus* prior to, and up to
145 10 years after, the onset of WNS. White-nose syndrome in bats was first observed in upstate

146 New York, at Howe's Cave during the winter of 2006-2007 (Blehert et al., 2009). Our historic
147 samples were obtained from individuals consisting of the eastern population of *M. lucifugus*
148 (Miller-Butterworth et al., 2014; Vonhof et al., 2015) from New York (NY) (from the first
149 batch of dead bats found at Howe's Cave in 2006) and from bats caught in central Pennsylvania
150 (PA) in 2005-2006 (Table 1.,Supp. Table 1.). Bats in PA became affected by the disease in
151 roughly 2008–2009. The remnants of the eastern North American population in NY and PA
152 were sampled again in 2016, and genetic diversity was compared before and after WNS (Table
153 1., Supp. Table 1.). We sampled wing tissue from frozen specimens of known origin (Supp.
154 Table 1.) that were collected and stored by the New York State Department of Environmental
155 Conservation (Delmar, NY) and D. Reeder to obtain Pre-WNS samples. Post-WNS bats were
156 captured using mist nets and harp traps during 2015 -2016. In addition to samples from PA and
157 NY, we also collected two samples from Upper-Peninsula Michigan (UPMI) for polymorphic
158 site selection (see Section 2.3.) to increase the diversity of sites for our samples. Tissue samples
159 were collected using either 3.0 mm or 5.0 mm biopsy punches (Integra Milltex, Plainsboro,
160 NJ) and stored in 95% ethanol until extraction. We extracted DNA using QIAmp DNA Mini
161 Kits (Qiagen, Hilden Germany) and stored DNA at -80°C until sequencing.

162 ### 2.3. Sequencing methods

163 Sequencing libraries were made for two sets of data: (1) Six individuals from PA (N = 2), NY
164 (N = 2) and UPMI (N= 2) in order to initially identify a set of polymorphic sites within the *M.*
165 *lucifugus* genome within the focal population (See Supp. Table 1. for information on
166 individuals). Individual sequencing increases the confidence of SNP discovery, relative to
167 pooled sequencing, since individuals exhibit discrete variation in the number of alleles they

168 carry at each potential SNP site; (2) Equimolar pools of DNA from multiple individuals from
169 within our north-eastern US population (NY and PA) at each of two timepoints (pre- and post-
170 WNS) to give four pooled sequencing libraries. TruSeq Nano libraries with a 350 bp insert size
171 were prepared from all samples and run on a HiSeq4000 platform to generate 2x 150 bp reads
172 providing ~15 Gbp of sequence data (~7.5x coverage) for each individual and ~90 Gbp of
173 sequence data (~45x coverage) for each pool. Adapter sequences were removed with Cutadapt
174 v1.2.1 and trimmed with Sickle 1.200 with a minimum quality score of 20.

175 ## 2.4. Bioinformatics methods

176 Reads from the six individuals were mapped onto the *M. lucifugus* reference genome
177 (https://www.broadinstitute.org/brown-bat/little-brown-bat-genome-project) using Bowtie2
178 v2.2.5 (Langmead and Salzberg, 2012), with the '—sensitive-local' preset. Reads were sorted
179 using SAMtools v1.1 (Li et al., 2009) and combined by read group (with duplicates removed
180 using a 'lenient' validation stringency setting) using Picard-tools v2.5.0
181 (http://broadinstitute.github.io/picard). SNPs were called across all six individuals with the
182 Genome Analysis Toolkit (GATK) v3.4 HaplotypeCaller (McKenna et al., 2010) using default
183 parameters. Within this SNP set, high-quality bivalent SNPs were selected that met selection
184 criteria across the six individuals (Quality Score > 100; AF<1; 30>=DP>=100) and were input
185 to the SAMtools mpileup function as a list of sites at which pileup was to be generated.

186 Reads from the pooled samples were mapped to the *M. lucifugus* reference genome as above
187 and SAMtools mpileup was used to count alleles at high-quality SNP sites identified above
188 (i.e. reads matching either the reference or alternate allele for bivalent loci). Sites with coverage
189 in the bottom 10% or top 10% quantiles summed across the pooled samples were excluded

190 (since these could reflect inaccuracies in the reference genome), leaving about 13.5 million
191 sites.

192 Average heterozygosity within the pooled samples was calculated using npstats (Ferretti et al.,
193 2013), which controls for number of individuals within each sequencing pool and sequencing
194 depth, thus allowing robust comparisons between pooled samples. One million SNPs were
195 randomly picked and permuted, with 1000 sets of 1000 SNPs used to calculate the observed
196 heterozygosity within each pooled set of individuals and, from these, we produced the median
197 and 95% confidence intervals on heterozygosity.

198 Using allele counts at each locus to estimate allele frequencies, F_{ST} was calculated without
199 weighting for sampling effort ($F_{ST} = \left(\bar{p}(1-\bar{p}) - \overline{p(1-p)}\right)/\bar{p}(1-\bar{p})$, where p is the allele
200 frequency and either averaged between populations ($\bar{p}$) or the value $p(1-p)$ averaged across
201 populations). F_{ST} was separately calculated between the Pre-WNS and Post-WNS samples and
202 between subsections thereof, specifically PA pre- vs post-WNS, NY pre- vs post-WNS, PA
203 pre- vs NY pre-WNS, PA post- vs NY post-WNS, and all PA vs all NY). Selection is expected
204 to elevate F_{ST} at specific genomic regions relative to background levels due to sampling noise
205 or genetic drift, which are expected to act equally across the genome. To identify such regions
206 across the genome, a moving window was applied to calculate median pairwise F_{ST} values for
207 groups of 500 consecutive SNPs at a time to even out sampling effects. Moving windows
208 shifted 100 SNPs at a time, thus providing the best balance between fine detail and practicality.
209 Allele frequency estimates were weighted by the number of individuals in each pool. This was
210 done using a custom R script (see Data availability section), run using R v3.4.1 (R
211 Development Core Team, 2011). Results were confirmed using Popoolation2 with a 10 kb

212 sliding window and with defined pool sizes. This gave the same qualitative results, but higher
213 levels of background noise (Kofler et al., 2011). Additionally, Popoolation2 was used to
214 perform Fishers Exact Tests on individual SNPs in order to test whether any very highly
215 significant SNPs were missed by the moving window approach.

216 From the comparison of the NY and PA pooled samples (i.e. the comparison that produced the
217 highest F_{ST} values), we visually identified across the whole genome windows with median F_{ST}
218 values greater than 5 standard deviations from the mean, as well as those with F_{ST} values greater
219 than 0.05, indicating at least 'moderate' genetic differentiation (Wright, 1978). The numbers
220 of such complete windows within gene models were counted for each gene to identify genes
221 potentially under selective pressure.

222 3. Results

223 3.1. Pre-WNS vs Post-WNS comparisons

224 To detect regions of the genome that may be under selection, we plotted F_{ST} across the *M.*
225 *lucifugus* genome, calculated from allele counts within moving windows covering 500 SNPs
226 and shifting 100 SNPs at a time. Comparing Pre- and Post-WNS samples revealed an overall
227 low level of population differentiation due to genetic structure (F_{ST} median of 0.0059; Table
228 2). Whilst a small number of windows have F_{ST} values slightly beyond our arbitrary cut-off of
229 5 standard deviations above the mean, none have F_{ST} values exceeding 0.05, suggesting that
230 there is not even moderate selection in any region of the genome in Post-WNS samples
231 compared to Pre-WNS samples (Fig. 2, Table 2)(Wright, 1978). Similarly, using Fisher exact
232 tests from Popoolation2 at a threshold of $p < 10^{-6}$, no individual SNPs were found to be
233 consistently associated with differences Pre- versus Post-WNS among the four sets of samples.

234 ### 3.2. Comparisons within US states

235 Due to our sampling and sequencing setup, we were also able to separately look at individuals
236 of the same population from two discrete geographical locations within their range. In our case
237 an arbitrary divide was made between bats sampled in NY and PA. Although population
238 genetic analysis based on a considerably lower number of genetic markers assigns *M. lucifugus*
239 on the eastern coast of North America to the same population (Vonhof et al., 2015), the species
240 shows high degrees of philopatry (Davis and Hitchcock, 1965; Norquay et al., 2013),
241 warranting the examination of these arbitrarily assigned pools of individuals outside the mean
242 dispersal range of the species using more accurate, whole-genome sequencing based population
243 genetic analyses.

244 A number of minor differences (F_{ST} > 5 stdevs above mean, but F_{ST} < 0.05) between these
245 arbitrary sets of samples are evident prior to arrival of WNS, as well as a peak in scaffold
246 GL429835 with an F_{ST} value exceeding 0.05 (Fig. 3a). The high peak consists of 4 windows
247 the midpoints of which span an 81,887 bp region within a coding sequence consisting of 47
248 exons, which encodes the NIPBL cohesion loading factor (NCBI Gene ID: 102430106). The
249 highest peak in a comparison of PA populations Pre- and Post-WNS (Fig. 3b) lies in a similar
250 position within this coding region, as does a peak in a similar comparison of NY samples (Fig.
251 3c), though neither exceed the F_{ST} value cut-off of 0.05.

252 ### 3.3. Post-WNS comparisons between US states

253 When comparing the Post-WNS individuals sampled from PA with the Post-WNS individuals
254 from NY, the peak on scaffold GL429835 is no longer visible, but a far more pronounced spike

255 in F_{ST} values can be clearly seen in scaffold GL429776 (Fig. 4a), indicating relatively large
256 allele frequency differences between the sample sets in this region of the genome. This is also
257 seen, to a lesser extent, when comparing all samples from NY with all samples from PA (Fig.
258 4b). However, this significant peak in this comparison of all samples collected does not affect
259 average fixation across the genome relative to the other comparison of all samples, Pre-WNS
260 vs Post-WNS (Table 2).

261 We examined scaffold GL429776 more closely to compare the F_{ST} values between individuals
262 from the arbitrarily selected sample sets from NY Post-WNS and PA Post-WNS (Fig. 4a).
263 Genes within scaffold GL429776 containing windows with fixation values > 0.05 between the
264 NY Post-WNS and PA Post-WNS samples, are presented in Table 4 and Fig. 4a.

265 To clarify why we saw no fixation at this site when comparing Pre-WNS and Post-WNS
266 populations (Fig. 3a), nor when we compared Pre-WNS samples from both geographical
267 origins (Figs. 3b and 3c), we calculated for the relevant subpopulations the proportion of
268 reference alleles called at each site included in the F_{ST} window analyses (Fig. 5). This revealed
269 a small decrease over time in the proportion of the reference alleles seen at this locus in the PA
270 subpopulation (Fig. 5a), commensurate with an increase in proportion of reference alleles in
271 the NY sample set (Fig. 5b). As such, existing differences between the NY and PA sample sets
272 were insufficient to cause a relative rise in fixation prior to WNS spreading through the
273 population (Fig 5c). Conversely, Post-WNS, allele proportions at this site in both sample sets
274 had not changed sufficiently to suggest selection *within* the sample set but demonstrated clear
275 differences *between* the NY and PA sample sets (Fig. 5d).

276 In the Post-WNS comparison, peaks which were above our arbitrary threshold of 5 standard
277 deviations above the mean across the whole genome, but below F_{ST} = 0.05, can also be
278 observed in small scaffolds on the right-hand side of the F_{ST} plots. The 63 windows comprising
279 these peaks lie in 47 scaffolds. Of these, high F_{ST} windows lie in only 6 protein-coding regions
280 across 6 scaffolds (Table 3). Two of these encode partial gene models. Of the 4 remaining
281 models containing high F_{ST} regions, all but 1 is described on NCBI as a "Low Quality Protein".
282 The exception is a gene encoding the ankyrin 2 protein, within which 7 high F_{ST} windows lie.

283 ### 3.4. Measures of heterozygosity within subpopulations

284 We examined heterozygosity across the genome in the subpopulations divided by time and
285 location to measure whether the epizootic reduces genetic diversity. We found the following
286 values: PA pre-WNS: Median: 0.263 (0.252 – 0.274 95% CI); PA post-WNS: 0.247 (0.239 –
287 0.255); NY pre-WNS: 0.255 (0.247 – 0.263); and NY post-WNS: 0.256 (0.247 -0.265).

288 ## 4. Discussion

289 Examining our data as a whole, we found low F_{ST} values between the Pre- and Post-WNS
290 individuals of our eastern North American *M. lucifugus* population, the absence of fixation
291 suggesting that WNS has not decreased the population in size sufficiently for the disease to
292 have an effect on genetic diversity. Also, we found no significant changes in within-population
293 heterozygosity Post-WNS, despite the massive population declines caused by WNS over the
294 past decade, and found overall high heterozygosity across the genome. These results are in
295 accordance with a similar, low-coverage study conducted by Gignoux-Wolfsohn et al. (2018).
296 Panmixia of populations in evolutionary time in bats to the east of the Rocky Mountains has

297 been previously documented (Vonhof et al., 2016; Wilder et al., 2015). Gignoux-Wolfsohn *et*
298 *al.* (2018) present evidence for a soft selective sweep, where selection acts on standing genetic
299 variation, between Pre- and Post-WNS populations. Their analysis is based on a change in
300 minor allele frequencies due to selection, distinguished from background demography using a
301 simulation approach; and it shows a complex picture of potentially up to 85 unlinked SNPs,
302 each exhibiting small effects and with little or no selective signal at adjacent SNPs. In contrast,
303 a recent case study of selection on standing genetic variation, by myxoma virus in rabbits,
304 showed that soft selective sweeps caused concerted changes in allele frequencies at sets of
305 linked SNPs around coding loci (Alves et al., 2019).

306 The species originally described as *M. lucifugus* in North America (Fenton and Barclay, 1980)
307 has since been divided into five non-sister species (Morales and Carstens, 2018). All of the
308 individuals sampled in our study belong to *M. lucifugus senso stricto*, with a range extending
309 from the east coast of North America to Alaska, and furthermore, to the same previously
310 assigned population (Miller-Butterworth et al., 2014). Previous nuclear genetic studies show
311 that differentiation is low, and there is no evidence for any major barriers to nuclear gene flow
312 across the range of *M. lucifugus*.

313 Due to our sampling design, we were able to separate bats geographically within our sampling
314 range. We made the arbitrary cut-off point for a more in-depth investigation of bats sampled in
315 the states of PA compared to NY. Here, we see low F_{ST} values between the two groups of bats
316 prior to the onset of WNS, indicating an absence of selection across the genome, with the
317 exception of a small peak in scaffold GL429835, which lies within a gene model encoding the
318 NIPBL cohesion loading factor. Relatively high F_{ST} values are also visible within this region

319 when comparing the PA population before and after the spread of WNS, as well as the NY
320 population pre- and post-WNS. However, this peak is not evident when comparing PA and NY
321 post-WNS (Fig. 4a). This suggests that this coding sequence was under selective pressures,
322 manifesting as different allelic fixations, in both subpopulations prior to the arrival of WNS,
323 but that any selection was nullified by the population-level impact of WNS (or another event
324 occurring during the same timeframe). The protein NIPBL, as described in a review by Peters
325 et al. (2008) plays an important role in the function of the cohesin complex, which is vital for
326 chromosome segregation, DNA damage repair, and gene expression regulation. As these
327 results suggest the loss of low-level functional diversity at this locus in our subpopulations, it
328 would be interesting to further investigate what impact this will have on the population as a
329 whole.

330 The F_{ST} comparison of Post-WNS individuals sampled from PA and NY depicts considerable
331 genetic differentiation within scaffold GL429776; differentiation which did not exist in the
332 Pre-WNS comparison of individuals sampled from these geographical areas. This is a
333 difference which would have gone unnoticed had we not made the arbitrary comparison
334 between bats sampled in NY and PA, or used fewer genetic markers instead of a whole-genome
335 approach (Miller-Butterworth et al., 2014; Vonhof et al., 2015). The region's appearance post-
336 WNS when considering all geographical locations together is not, however, reflected when the
337 data are broken down into representatives of each state. A comparison of allele frequencies of
338 individual SNPs within this region shows that individuals sampled from PA showed an increase
339 in deviation from the reference genome over time, whilst a greater proportion of reference
340 alleles were seen in NY samples Post-WNS compared with Pre-WNS. The differences in

341 proportions, growing as they were over time, were insufficient to exhibit a high fixation value
342 Pre-WNS, but were notably different after the disease had spread through the population.

343 This region within the scaffold containing the peak contains six annotated genes with very
344 different functions. Two, POC1B and CEP290, are involved in cilia development and
345 maintenance. The ATP2B1 gene encodes a protein which belongs to the family of P-type
346 primary ion transport ATPases, whereas TMTC3 is involved in the control of endoplasmic
347 reticulum stress response. MGAT4C is a glycosyltransferase that participates in the transfer of
348 N-acetylglucosamine (GlcNAc) to the core mannose residues of N-linked glycans. Finally,
349 KITLG produces a protein involved in mast cell development, migration and function, and
350 melanogenesis. KITLG has been documented as a target of evolution in recent studies and in
351 humans it has been linked with thermoregulation (Yang et al., 2018), which is a critical
352 component of bat life history (Studier and O'Farrell, 1972). In fact, upregulation of KITLG at
353 low temperature helps promote the production of brown fat for heat generation (Huang et al.,
354 2014). Bats utilise brown adipose tissue in arousals to normothermia from different degrees of
355 torpor (Thomas et al., 1990). There is also evidence of parallel evolution of pigmentation in
356 sticklebacks and humans linked to KITLG (Miller et al., 2007), as well as its role in determining
357 resistance/susceptibility to swine respiratory diseases in Erhulian pigs (Huang et al., 2017).
358 KITLG, by influencing mast cell development, could also play a role in either protective or
359 pathological immune responses to *P. destructans*, which may involve IgE-mediated
360 recognition of secreted fungal proteins. As such, temporal changes we found in allele
361 frequencies at this locus could, for instance, be linked to differences in hibernation site
362 temperatures, and/or thermoregulatory needs in bats sampled at different locations (Humphries
363 et al., 2002; Thomas et al., 1990). Spatial patterns, as seen here between the arbitrarily pooled

364 samples from PA and NY, could be due to local adaptation, in which strong selective sweeps
365 may be linked to gene variants favoured in local interactions (Hansen et al., 2012; Kyle et al.,
366 2014; Rico et al., 2015; Schoville et al., 2012). Whilst we lack data concerning migration
367 patterns of the bats studied here, as well as the environmental conditions within their
368 microfugia, future work would benefit from these data in a bid to understand whether bats
369 repeatedly frequent habitats with similar conditions and whether, indeed, there is a significant
370 difference in conditions across these Eastern states that explains the rapid rise in fixation at this
371 locus.

372 The increase in F_{ST} values in this scaffold GL429776 could, alternatively, be due to the massive
373 population decline caused by WNS (Langwig et al., 2017). Although not supported by existing
374 data, the decline could potentially have resulted in a decrease in connectivity and gene flow
375 between remnant local populations allowing for a local adaptation to arise (Bohonak, 1999;
376 Lilley, Anttila, & Ruokolainen, 2018). Genetically resolved examples of local adaptations are
377 rare (Hoekstra et al., 2006) and, in our focal system, pinpointing the causality leading to local
378 adaptation is especially difficult due to the cryptic life history of bats. Determining how these
379 variants are spread or localised among populations is essential to understanding and managing
380 the emergence of new selective pressures (Eizaguirre et al., 2012; Kyle et al., 2014).

381 The ankyrin 2 protein encoding gene, lying within the observed small scaffolds on the right-
382 hand side of the F_{ST} plots has a wide range of attributed Gene Ontology functions (The UniProt
383 Consortium, 2019), which reinforce the ubiquitous nature and far-reaching roles of ankyrin-
384 repeat-containing genes across organisms (Voronin and Kiseleva, 2007). Alternatively, the
385 peaks in this area may have arisen because only relatively few SNPs were called there given

386 the small size of the scaffolds, thus limiting our ability to generate high-quality windows, hence
387 the greater sampling noise.

388 We cannot fully exclude the possibility of WNS selecting for alleles in our scaffold of interest
389 through. It is likely that there is concurrent selection occurring across multiple populations,
390 and that selection is not acting to the same degree or even on the same loci in different
391 geographic areas affected by WNS (Messer and Petrov, 2013). This also applies to interpreting
392 the results on a smaller scale: the samples had not been collected from exactly the same
393 locations before and after WNS, which may contribute to our results. Individuals sampled
394 during the winter, at their hibernacula, may not inhabit the vicinity of these locations during
395 the summer, although dispersal distances are often short (Davis & Hitchcock, 1965; but see
396 Norquay et al., 2013).

397 Despite not seeing a genetic signal associated with resistance in *M. lucifugus*, remnant
398 populations appear to be surviving year after year and even increasing in size notwithstanding
399 infection loads during the hibernation period (Langwig et al., 2017; Lilley et al., 2016). The
400 fact that the intensity of infection with *P. destructans* appears to be significantly lower for
401 remnant populations compared to colonies in the midst of the epidemic phase and massive
402 declines may suggest the development of resistance in these populations (Bernard et al., 2017;
403 Langwig et al., 2017). However, the role of environmental interactions during the hibernation
404 period, when the bat hosts are most vulnerable to the pathogen, have been largely neglected,
405 although the effect of humidity and temperature on the growth of the fungal pathogen and
406 survival of the host have been separately studied (Grieneisen et al., 2015; Marroquin et al.,
407 2017; Verant et al., 2012). Modelling also suggests that environmental factors, including the

408 cave microbiome, have an impact on the proliferation and infectivity of *P. destructans*
409 (Hayman, Pulliam, Marshall, Cryan, & Webb, 2016; Lilley et al., 2018). This is supported by
410 the discovery of microbes in hibernacula environments and bats that are able to retard the
411 growth of the fungus (Micalizzi et al., 2017; Zhang et al., 2014, 2015). In light of our results
412 and considering bat life history as a whole, adaptation and evolutionary rescue may not be a
413 fast track for recovery of bat populations affected by WNS (Maslo and Fefferman, 2015). More
414 likely the variability in hibernation site environmental conditions and strong selection for
415 microbial taxa that inhibit *P. destructans* could explain why populations are recovering from
416 the zoonosis (Cheng et al., 2016; Lemieux-Labonté, Simard, Willis, & Lapointe, 2017; Lilley
417 et al., 2018).

418 It is still unclear how frequently genetic adaptation occurs in natural populations and under
419 what circumstances it is promoted (Schoville et al., 2012). Many studies have recorded
420 phenotypic changes in natural populations and attributed them to host-pathogen interactions
421 (Frank et al., 2014; Kilpatrick, 2006; Langwig et al., 2017; Råberg et al., 2009). However, it is
422 difficult to determine conclusively whether changes in phenotype are the result of selection in
423 the genome or a result of phenotypic plasticity (Paterson et al., 2010; Routtu and Ebert, 2015).
424 Also, the assumed benefit of change (i.e. adaptation) is often not tested experimentally, which
425 would allow for inference of causality with the pathogen through exclusion of other potential
426 drivers.

427 To conclude, our results suggest WNS has not yet subjected populations of *M. lucifugus* to
428 selective pressures leading to genetic adaptation in remnant populations. No signs of selection
429 in comparisons of genomes of Pre-WNS and ten years Post-WNS populations were observed,

430 although recent research has produced contradicting results (Donaldson et al., 2017; Gignoux-
431 Wolfsohn et al., 2018). As for our results, this is something that is not unexpected with a species
432 in which the effective population size most likely numbered in tens of millions of individuals
433 prior to the onset of WNS. Our results indicate that the existence and recent growth of remnant
434 populations of *M. lucifugus* are more likely attributable to other factors, such as microbiome
435 adaptation and hibernation site selection among others, rather than genetic adaption. However,
436 we found increased variability in a specific area of the genome in a comparison of Post-WNS
437 samples from our two different study states, relative to Pre-WNS samples. We suggest this is
438 due to weakened connectivity between bats at different locations allowing for local adaptations
439 to enrich in the absence of gene flow. Although genes in the high F_{ST} region of the genome
440 were identified, and genes such as KITLG provide interesting avenues of research, further
441 investigation into the processes in bat life history to which these genes are related are required
442 to expound upon the existing gene annotations.

443 ## Acknowledgements

444 We thank Svenska Kulturfonden, H2020 Marie Skłodowska-Curie Actions (TML, 706196)
445 and the Natural Environment Research Council, UK for funding the study; staff at the Centre
446 for Genomic Research, University of Liverpool, UK for DNA sequencing expertise; Jenni
447 Prokkola and Riley F. Bernard for proofreading the manuscript; and Alice Lilley, Cali Wilson,
448 Beth Rogers and Mike Scafini for assisting in sample collection.

449 ## Author contributions

450 TML and SP designed the research. TML, DMR, KAF, AK, GGR and CH collected the
451 samples. TML prepared samples for sequencing. TML, IWW and SP analysed the data. TML,

452 IWW and SP wrote the first draft of the manuscript, and all authors contributed to the final
453 version.

454 Data availability statement

455 Raw data are available at ENA accession XXXXX and bioinformatics code at
456 https://github.com/scottishwormboy/myoluc.

457 References

458 Alves, J.M., Carneiro, M., Cheng, J.Y., Matos, A.L. de, Rahman, M.M., Loog, L., Campos,
459 P.F., Wales, N., Eriksson, A., Manica, A., et al. (2019). Parallel adaptation of rabbit populations
460 to myxoma virus. Science *363*, 1319–1326.

461 Ange-Stark, M., Cheng, T.L., Hoyt, J.R., Langwig, K.E., Parise, K.L., Frick, W.F., Kilpatrick,
462 A.M., MacManes, M.D., and Foster, J.T. (2019). White-nose syndrome restructures bat skin
463 microbiomes. BioRxiv 614842.

464 Bernard, R.F., and McCracken, G.F. (2017). Winter behavior of bats and the progression of
465 white-nose syndrome in the southeastern United States. Ecol. Evol. *7*, 1487–1496.

466 Bernard, R.F., Willcox, E.V., Parise, K.L., Foster, J.T., and McCracken, G.F. (2017). White-
467 nose syndrome fungus, Pseudogymnoascus destructans, on bats captured emerging from caves
468 during winter in the southeastern United States. BMC Zool. *2*, 12.

469 Blehert, D.S., Hicks, A.C., Behr, M., Meteyer, C.U., Berlowski-Zier, B.M., Buckles, E.L.,
470 Coleman, J.T.H., Darling, S.R., Gargas, A., Niver, R., et al. (2009). Bat white-nose syndrome:
471 an emerging fungal pathogen? Science *323*, 227–227.

472 Bohonak, A.J. (1999). Dispersal, gene flow, and population structure. Q. Rev. Biol. *74*, 21–45.

473 Boots, M., Best, A., Miller, M.R., and White, A. (2009). The role of ecological feedbacks in
474 the evolution of host defence: what does theory tell us? Philos. Trans. R. Soc. Lond. B Biol.
475 Sci. *364*, 27–36.

476 Campana, M., Kurata, N., Foster, J.T., Helgen, L., Reeder, D., Fleischer, R., and Helgen, K.M.
477 (2017). White-nose syndrome fungus in a 1918 bat specimen from France. Emerg. Infect. Dis.
478 J. *23*, 1–1.

479 Campbell, M.C., and Tishkoff, S.A. (2008). African Genetic Diversity: Implications for
480 Human Demographic History, Modern Human Origins, and Complex Disease Mapping. Annu.
481 Rev. Genomics Hum. Genet. *9*, 403–433.

482 Carlson, S.M., Cunningham, C.J., and Westley, P.A.H. (2014). Evolutionary rescue in a
483 changing world. Trends Ecol. Evol. *29*, 521–530.

484 Cheng, T.L., Mayberry, H., McGuire, L.P., Hoyt, J.R., Langwig, K.E., Nguyen, H., Parise,
485 K.L., Foster, J.T., Willis, C.K.R., Kilpatrick, A.M., et al. (2016). Efficacy of a probiotic
486 bacterium to treat bats affected by the disease white-nose syndrome. J. Appl. Ecol. *54*, 701–
487 708.

488 Cheng, T.L., Gerson, A., Moore, M.S., Reichard, J.D., DeSimone, J., Willis, C.K.R., Frick,
489 W.F., and Kilpatrick, A.M. (2019). Higher fat stores contribute to persistence of little brown
490 bat populations with white-nose syndrome. J. Anim. Ecol. *0*.

491 Cryan, P.M., Meteyer, C.U., Boyles, J.G., and Blehert, D.S. (2010). Wing pathology of white-
492 nose syndrome in bats suggests life-threatening disruption of physiology. Bmc Biol. *8*, 135.

493 Cryan, P.M., Meteyer, C.U., Blehert, D.S., Lorch, J.M., Reeder, D.M., Turner, G.G., Webb, J.,
494 Behr, M., Verant, M., Russe, R.E., et al. (2013). Electrolyte depletion in white-nose syndrome
495 bats. J. Wildl. Dis. *49*, 398–402.

496 Daszak, P., Berger, L., Cunningham, A.A., Hyatt, A.D., Green, D.E., and Speare, R. (1999).
497 Emerging infectious diseases and amphibian population declines. Emerg. Infect. Dis. *5*, 735–
498 748.

499 Daszak, P., Cunningham, A.A., and Hyatt, A.D. (2000). Emerging infectious diseases of
500 wildlife-threats to biodiversity and human health. Science *287*, 443–449.

501 Davis, W.H., and Hitchcock, H.B. (1965). Biology and migration of the bat, *Myotis lucifugus*,
502 in New England. J. Mammal. *46*, 296–313.

503 Davy, C.M., Donaldson, M.E., Rico, Y., Lausen, C.L., Dogantzis, K., Ritchie, K., Willis,
504 C.K.R., Burles, D.W., Jung, T.S., McBurney, S., et al. (2017a). Prelude to a panzootic: Gene
505 flow and immunogenetic variation in northern little brown myotis vulnerable to bat white-nose
506 syndrome. FACETS.

507 Davy, C.M., Donaldson, M.E., Willis, C.K.R., Saville, B.J., McGuire, L.P., Mayberry, H.,
508 Wilcox, A., Wibbelt, G., Misra, V., Bollinger, T., et al. (2017b). The other white-nose
509 syndrome transcriptome: Tolerant and susceptible hosts respond differently to the pathogen
510 Pseudogymnoascus destructans. Ecol. Evol. 7161–7170.

511 De Castro, F., and Bolker, B. (2005). Mechanisms of disease-induced extinction. Ecol. Lett. *8*,
512 117–126.

513 Deschamps, M., Laval, G., Fagny, M., Itan, Y., Abel, L., Casanova, J.-L., Patin, E., and
514 Quintana-Murci, L. (2016). Genomic Signatures of Selective Pressures and Introgression from
515 Archaic Hominins at Human Innate Immunity Genes. Am. J. Hum. Genet. *98*, 5–21.

516 Di Gaspero, G., Copetti, D., Coleman, C., Castellarin, S.D., Eibach, R., Kozma, P., Lacombe,
517 T., Gambetta, G., Zvyagin, A., Cindrić, P., et al. (2012). Selective sweep at the Rpv3 locus
518 during grapevine breeding for downy mildew resistance. TAG Theor. Appl. Genet. Theor.
519 Angew. Genet. *124*, 277–286.

520 Dobony, C.A., and Johnson, J.B. (2018). Observed resiliency of little brown myotis to long-
521 term white-nose syndrome exposure. J. Fish Wildl. Manag. *9*, 168–179.

522 Donaldson, M.E., Davy, C.M., Willis, C.K.R., McBurney, S., Park, A., and Kyle, C.J. (2017).
523 Profiling the immunome of little brown myotis provides a yardstick for measuring the genetic
524 response to white-nose syndrome. Evol. Appl. *10*, 1076–1090.

525 Eizaguirre, C., Lenz, T.L., Kalbe, M., and Milinski, M. (2012). Divergent selection on locally
526 adapted major histocompatibility complex immune genes experimentally proven in the field.
527 Ecol. Lett. *15*, 723–731.

528 Fenton, M.B., and Barclay, R.M.R. (1980). *Myotis lucifugus*. Mamm. Species 1–8.

529 Ferretti, L., Ramos-Onsins, S.E., and Pérez-Enciso, M. (2013). Population genomics from pool
530 sequencing. Mol. Ecol. *22*, 5561–5576.

Field, K.A., Johnson, J., Lilley, T., Reeder, S., Rogers, E., Behr, M., and Reeder, D. (2015). The white-nose syndrome transcriptome: activation of anti-fungal host responses in wing tissue of hibernating bats. Plos Pathog. *11*, e1005168.

Field, K.A., Sewall, B.J., Prokkola, J.M., Turner, G.G., Gagnon, M., Lilley, T.M., White, J.P., Johnson, J.S., Hauer, C.L., and Reeder, D.M. (2018). Effect of torpor on host transcriptomic responses to a fungal pathogen in hibernating bats. Mol. Ecol.

Frank, C.L., Michalski, A., McDonough, A.A., Rahimian, M., Rudd, R.J., and Herzog, C. (2014). The resistance of a North American bat species (Eptesicus fuscus) to White-Nose Syndrome (WNS). PLoS ONE *9*, e113958.

Frick, W.F., Pollock, J.F., Hicks, A.C., Langwig, K.E., Reynolds, D.S., Turner, G.G., Butchkoski, C.M., and Kunz, T.H. (2010). An Emerging disease causes regional population collapse of a common North American bat species. Science *329*, 679–682.

Frick, W.F., Puechmaille, S.J., Hoyt, J.R., Nickel, B.A., Langwig, K.E., Foster, J.T., Barlow, K.E., Bartonička, T., Feller, D., Haarsma, A.-J., et al. (2015). Disease alters macroecological patterns of North American bats. Glob. Ecol. Biogeogr. *24*, 741–749.

Frick, W.F., Cheng, T.L., Langwig, K.E., Hoyt, J.R., Janicki, A.F., Parise, K.L., Foster, J.T., and Kilpatrick, A.M. (2017). Pathogen dynamics during invasion and establishment of white-nose syndrome explain mechanisms of host persistence. Ecology *98*, 624–631.

Gallana, M., Ryser-Degiorgis, M.-P., Wahli, T., and Segner, H. (2013). Climate change and infectious diseases of wildlife: Altered interactions between pathogens, vectors and hosts. Curr. Zool. *59*, 427–437.

552 Gignoux-Wolfsohn, S.A., Pinsky, M.L., Kerwin, K., Herzog, C., Hall, M., Bennett, A.B.,
553 Fefferman, N.H., and Maslo, B. (2018). Genomic signatures of evolutionary rescue in bats
554 surviving white-nose syndrome. BioRxiv 470294.

555 Grieneisen, L.E., Brownlee-Bouboulis, S.A., Johnson, J.S., and Reeder, D.M. (2015). Sex and
556 hibernaculum temperature predict survivorship in white-nose syndrome affected little brown
557 myotis (Myotis lucifugus). R. Soc. Open Sci. *2*, 140470.

558 Groot, N.G. de, Otting, N., Doxiadis, G.G.M., Balla-Jhagjhoorsingh, S.S., Heeney, J.L., Rood,
559 J.J. van, Gagneux, P., and Bontrop, R.E. (2002). Evidence for an ancient selective sweep in the
560 MHC class I gene repertoire of chimpanzees. Proc. Natl. Acad. Sci. *99*, 11748–11753.

561 Hansen, M.M., Olivieri, I., Waller, D.M., and Nielsen, E.E. (2012). Monitoring adaptive
562 genetic responses to environmental change. Mol. Ecol. *21*, 1311–1329.

563 Harazim, M., Horáček, I., Jakešová, L., Luermann, K., Moravec, J.C., Morgan, S., Pikula, J.,
564 Sosík, P., Vavrušová, Z., Zahradníková, A., et al. (2018). Natural selection in bats with
565 historical exposure to white-nose syndrome. BMC Zool. *3*, 8.

566 Hayman, D.T.S., Pulliam, J.R.C., Marshall, J.C., Cryan, P.M., and Webb, C.T. (2016).
567 Environment, host, and fungal traits predict continental-scale white-nose syndrome in bats. Sci.
568 Adv. *2*, e1500831.

569 Hoekstra, H.E., Hirschmann, R.J., Bundey, R.A., Insel, P.A., and Crossland, J.P. (2006). A
570 single amino acid mutation contributes to adaptive beach mouse color pattern. Science *313*,
571 101–104.

572 Huang, X., Huang, T., Deng, W., Yan, G., Qiu, H., Huang, Y., Ke, S., Hou, Y., Zhang, Y.,
573 Zhang, Z., et al. (2017). Genome-wide association studies identify susceptibility loci affecting
574 respiratory disease in Chinese Erhualian pigs under natural conditions. Anim. Genet. *48*, 30–
575 37.

576 Huang, Z., Ruan, H.-B., Xian, L., Chen, W., Jiang, S., Song, A., Wang, Q., Shi, P., Gu, X., and
577 Gao, X. (2014). The stem cell factor/Kit signalling pathway regulates mitochondrial function
578 and energy expenditure. Nat. Commun. *5*, 4282.

579 Humphries, M.M., Thomas, D.W., and Speakman, J.R. (2002). Climate-mediated energetic
580 constraints on the distribution of hibernating mammals. Nature *418*, 313–316.

581 Jeffery, K.J., and Bangham, C.R. (2000). Do infectious diseases drive MHC diversity?
582 Microbes Infect. *2*, 1335–1341.

583 Johnson, J.S., Reeder, D.M., McMichael, J.W., Meierhofer, M.B., Stern, D.W.F., Lumadue,
584 S.S., Sigler, L.E., Winters, H.D., Vodzak, M.E., Kurta, A., et al. (2014). Host, pathogen, and
585 environmental characteristics predict white-nose syndrome mortality in captive little brown
586 myotis (*Myotis lucifugus*). Plos One *9*, e112502.

587 Karlsson, E.K., Kwiatkowski, D.P., and Sabeti, P.C. (2014). Natural selection and infectious
588 disease in human populations. Nat. Rev. Genet. *15*, 379–393.

589 Kilpatrick, A.M. (2006). Facilitating the evolution of resistance to avian malaria in Hawaiian
590 birds. Biol. Conserv. *128*, 475–485.

591 Kofler, R., Pandey, R.V., and Schlötterer, C. (2011). PoPoolation2: identifying differentiation
592 between populations using sequencing of pooled DNA samples (Pool-Seq). Bioinformatics *27*,
593 3435–3436.

594 Kyle, C.J., Rico, Y., Castillo, S., Srithayakumar, V., Cullingham, C.I., White, B.N., and Pond,
595 B.A. (2014). Spatial patterns of neutral and functional genetic variations reveal patterns of local
596 adaptation in raccoon (Procyon lotor) populations exposed to raccoon rabies. Mol. Ecol. *23*,
597 2287–2298.

598 Langmead, B., and Salzberg, S.L. (2012). Fast gapped-read alignment with Bowtie 2. Nat.
599 Methods *9*, 357–359.

600 Langwig, K.E., Frick, W.F., Reynolds, R., Parise, K.L., Drees, K.P., Hoyt, J.R., Cheng, T.L.,
601 Kunz, T.H., Foster, J.T., and Kilpatrick, A.M. (2015). Host and pathogen ecology drive the
602 seasonal dynamics of a fungal disease, white-nose syndrome. Proc. R. Soc. B-Biol. Sci. *282*,
603 20142335.

604 Langwig, K.E., Hoyt, J.R., Parise, K.L., Frick, W.F., Foster, J.T., and Kilpatrick, A.M. (2017).
605 Resistance in persisting bat populations after white-nose syndrome invasion. Phil Trans R Soc
606 B *372*, 20160044.

607 Lemieux-Labonté, V., Simard, A., Willis, C.K.R., and Lapointe, F.-J. (2017). Enrichment of
608 beneficial bacteria in the skin microbiota of bats persisting with white-nose syndrome.
609 Microbiome *5*, 115.

610 Li, H., Handsaker, B., Wysoker, A., Fennell, T., Ruan, J., Homer, N., Marth, G., Abecasis, G.,
611 Durbin, R., and 1000 Genome Project Data Processing Subgroup (2009). The Sequence
612 Alignment/Map format and SAMtools. Bioinforma. Oxf. Engl. *25*, 2078–2079.

613 Lilley, T., Anttila, J., and Ruokolainen, L. (2018). Landscape structure and ecology influence
614 the spread of a bat fungal disease. Funct. Ecol. *0*.

615 Lilley, T.M., Johnson, J.S., Ruokolainen, L., Rogers, E.J., Wilson, C., Schell, S.M., Field,
616 K.A., and Reeder, D.M. (2016). White-nose syndrome survivors do not exhibit frequent
617 arousals associated with *Pseudogymnoascus destructans* infection. Front. Zool. *13*, 12.

618 Lilley, T.M., Prokkola, J.M., Johnson, J.S., Rogers, E.J., Gronsky, S., Kurta, A., Reeder, D.M.,
619 and Field, K.A. (2017). Immune responses in hibernating little brown myotis (*Myotis lucifugus*)
620 with white-nose syndrome. Proc R Soc B *284*, 20162232.

621 Lips, K.R., Brem, F., Brenes, R., Reeve, J.D., Alford, R.A., Voyles, J., Carey, C., Livo, L.,
622 Pessier, A.P., and Collins, J.P. (2006). Emerging infectious disease and the loss of biodiversity
623 in a Neotropical amphibian community. Proc. Natl. Acad. Sci. U. S. A. *103*, 3165–3170.

624 Lorch, J.M., Meteyer, C.U., Behr, M.J., Boyles, J.G., Cryan, P.M., Hicks, A.C., Ballmann,
625 A.E., Coleman, J.T.H., Redell, D.N., Reeder, D.M., et al. (2011). Experimental infection of
626 bats with *Geomyces destructans* causes white-nose syndrome. Nature *480*, 376-U129.

627 Lorch, J.M., Muller, L.K., Russell, R.E., O'Connor, M., Lindner, D.L., and Blehert, D.S.
628 (2013). Distribution and environmental persistence of the causative agent of white-nose
629 syndrome, *Geomyces destructans*, in bat hibernacula of the Eastern United States. Appl.
630 Environ. Microbiol. *79*, 1293–1301.

631 Luikart, G., Allendorf, F.W., Cornuet, J.-M., and Sherwin, W.B. (1998). Distortion of allele
632 frequency distributions provides a test for recent population bottlenecks. J. Hered. *89*, 238–
633 247.

634 Luis, A.D., and Hudson, P.J. (2006). Hibernation patterns in mammals: a role for bacterial
635 growth? Funct. Ecol. *20*, 471–477.

636 Marroquin, C.M., Lavine, J.O., and Windstam, S.T. (2017). Effect of Humidity on
637 Development of Pseudogymnoascus destructans, the Causal Agent of Bat White-Nose
638 Syndrome. Northeast. Nat. *24*, 54–64.

639 Maslo, B., and Fefferman, N.H. (2015). A case study of bats and white-nose syndrome
640 demonstrating how to model population viability with evolutionary effects. Conserv. Biol. *29*,
641 1176–1185.

642 Maslo, B., Valent, M., Gumbs, J.F., and Frick, W.F. (2015). Conservation implications of
643 ameliorating survival of little brown bats with white-nose syndrome. Ecol. Appl. *25*, 1832–
644 1840.

645 McGuire, L.P., Mayberry, H.W., and Willis, C.K.R. (2017). White-nose syndrome increases
646 torpid metabolic rate and evaporative water loss in hibernating bats. Am. J. Physiol.-Regul.
647 Integr. Comp. Physiol. *313*, R680–R686.

648 McKenna, A., Hanna, M., Banks, E., Sivachenko, A., Cibulskis, K., Kernytsky, A., Garimella,
649 K., Altshuler, D., Gabriel, S., Daly, M., et al. (2010). The Genome Analysis Toolkit: a
650 MapReduce framework for analyzing next-generation DNA sequencing data. Genome Res. *20*,
651 1297–1303.

652 Messer, P.W., and Petrov, D.A. (2013). Population genomics of rapid adaptation by soft
653 selective sweeps. Trends Ecol. Evol. *28*, 659–669.

654 Meteyer, C.U., Barber, D., and Mandl, J.N. (2012). Pathology in euthermic bats with white
655 nose syndrome suggests a natural manifestation of immune reconstitution inflammatory
656 syndrome. Virulence *3*, 583–588.

657 Micalizzi, E.W., Mack, J.N., White, G.P., Avis, T.J., and Smith, M.L. (2017). Microbial
658 inhibitors of the fungus *Pseudogymnoascus destructans*, the causal agent of white-nose
659 syndrome in bats. PLOS ONE *12*, e0179770.

660 Miller, C.T., Beleza, S., Pollen, A.A., Schluter, D., Kittles, R.A., Shriver, M.D., and Kingsley,
661 D.M. (2007). Cis-regulatory changes in Kit ligand expression and parallel evolution of
662 pigmentation in sticklebacks and humans. Cell *131*, 1179–1189.

663 Miller-Butterworth, C.M., Vonhof, M.J., Rosenstern, J., Turner, G.G., and Russell, A.L.
664 (2014). Genetic structure of little brown bats (Myotis lucifugus) corresponds with spread of
665 white-nose syndrome among hibernacula. J. Hered. esu012.

666 Minnis, A.M., and Lindner, D.L. (2013). Phylogenetic evaluation of Geomyces and allies
667 reveals no close relatives of Pseudogymnoascus destructans, comb. nov., in bat hibernacula of
668 eastern North America. Fungal Biol. *117*, 638–649.

669 Morales, A.E., and Carstens, B.C. (2018). Evidence that Myotis lucifugus "Subspecies" are
670 Five Nonsister Species, Despite Gene Flow. Syst. Biol. *67*, 756–769.

671 Norquay, K.J.O., Martinez-Nuñez, F., Dubois, J.E., Monson, K.M., and Willis, C.K.R. (2013).
672 Long-distance movements of little brown bats (Myotis lucifugus). J. Mammal. *94*, 506–515.

673 Paterson, S., Wilson, K., and Pemberton, J.M. (1998). Major histocompatibility complex
674 variation associated with juvenile survival and parasite resistance in a large unmanaged
675 ungulate population (Ovis aries L.). Proc. Natl. Acad. Sci. *95*, 3714–3719.

676 Paterson, S., Vogwill, T., Buckling, A., Benmayor, R., Spiers, A.J., Thomson, N.R., Quail, M.,
677 Smith, F., Walker, D., Libberton, B., et al. (2010). Antagonistic coevolution accelerates
678 molecular evolution. Nature *464*, 275–278.

679 Peters, J.-M., Tedeschi, A., and Schmitz, J. (2008). The cohesin complex and its roles in
680 chromosome biology. Genes Dev. *22*, 3089–3114.

681 Puechmaille, S.J., Wibbelt, G., Korn, V., Fuller, H., Forget, F., Mühldorfer, K., Kurth, A.,
682 Bogdanowicz, W., Borel, C., Bosch, T., et al. (2011). Pan-European distribution of white-nose
683 syndrome fungus (*Geomyces destructans*) not associated with mass mortality. PLoS ONE *6*,
684 e19167.

685 R Development Core Team (2011). R: A language and environment for statistical computing.

686 Råberg, L., Graham, A.L., and Read, A.F. (2009). Decomposing health: tolerance and
687 resistance to parasites in animals. Philos. Trans. R. Soc. Lond. B. Biol. Sci. *364*, 37–49.

688 Reeder, D.M., Frank, C.L., Turner, G.G., Meteyer, C.U., Kurta, A., Britzke, E.R., Vodzak,
689 M.E., Darling, S.R., Stihler, C.W., Hicks, A.C., et al. (2012). Frequent arousal from hibernation

690 linked to severity of infection and mortality in bats with white-nose syndrome. Plos One *7*,
691 e38920.

692 Ren, P., Haman, K.H., Last, L.A., Rajkumar, S.S., Keel, M.K., and Chaturvedi, V. (2012).
693 Clonal Spread of Geomyces destructans among Bats, Midwestern and Southern United States.
694 Emerg. Infect. Dis. *18*, 883–885.

695 Rico, Y., Morris-Pocock, J., Zigouris, J., Nocera, J.J., and Kyle, C.J. (2015). Lack of Spatial
696 Immunogenetic Structure among Wolverine (Gulo gulo) Populations Suggestive of Broad
697 Scale Balancing Selection. PLOS ONE *10*, e0140170.

698 van Riper, C., van Riper, S.G., Goff, M.L., and Laird, M. (1986). The Epizootiology and
699 Ecological Significance of Malaria in Hawaiian Land Birds. Ecol. Monogr. *56*, 327–344.

700 Robinson, S.J., Samuel, M.D., Johnson, C.J., Adams, M., and McKenzie, D.I. (2012).
701 Emerging prion disease drives host selection in a wildlife population. Ecol. Appl. Publ. Ecol.
702 Soc. Am. *22*, 1050–1059.

703 Routtu, J., and Ebert, D. (2015). Genetic architecture of resistance in *Daphnia* hosts against
704 two species of host-specific parasites. Heredity *114*, 241–248.

705 Scholthof, K.-B.G. (2007). The disease triangle: pathogens, the environment and society. Nat.
706 Rev. Microbiol. *5*, 152–156.

707 Schoville, S.D., Bonin, A., François, O., Lobreaux, S., Melodelima, C., and Manel, S. (2012).
708 Adaptive Genetic Variation on the Landscape: Methods and Cases. Annu. Rev. Ecol. Evol.
709 Syst. *43*, 23–43.

710 Sironi, M., Cagliani, R., Forni, D., and Clerici, M. (2015). Evolutionary insights into host–
711 pathogen interactions from mammalian sequence data. Nat. Rev. Genet. *16*, 224–236.

712 Smith, K.F., Sax, D.F., and Lafferty, K.D. (2006). Evidence for the Role of Infectious Disease
713 in Species Extinction and Endangerment. Conserv. Biol. *20*, 1349–1357.

714 Sparks, A.M., Watt, K., Sinclair, R., Pilkington, J.G., Pemberton, J.M., McNeilly, T.N.,
715 Nussey, D.H., and Johnston, S.E. (2019). The genetic architecture of helminth-specific immune
716 responses in a wild population of Soay sheep (Ovis aries). BioRxiv 628271.

717 Spurgin, L.G., and Richardson, D.S. (2010). How pathogens drive genetic diversity: MHC,
718 mechanisms and misunderstandings. Proc. Biol. Sci. *277*, 979–988.

719 Studier, E.H., and O'Farrell, M.J. (1972). Biology of Myotis thysanodes and M. lucifugus
720 (Chiroptera: Vespertilionidae). I. Thermoregulation. Comp. Biochem. Physiol. A *41*, 567–595.

721 Teacher Amber G. F., Garner Trenton W. J., and Nichols Richard A. (2009). Population genetic
722 patterns suggest a behavioural change in wild common frogs (Rana temporaria) following
723 disease outbreaks (Ranavirus). Mol. Ecol. *18*, 3163–3172.

724 The UniProt Consortium (2019). UniProt: a worldwide hub of protein knowledge. Nucleic
725 Acids Res. *47*, D506–D515.

726 Thomas, D.W., Dorais, M., and Bergeron, J.-M. (1990). Winter Energy Budgets and Cost of
727 Arousals for Hibernating Little Brown Bats, Myotis lucifugus. J. Mammal. *71*, 475–479.

728 Tompkins, D.M., Carver, S., Jones, M.E., Krkošek, M., and Skerratt, L.F. (2015). Emerging
729 infectious diseases of wildlife: a critical perspective. Trends Parasitol. *31*, 149–159.

730 Turner, G.G., Reeder, D.M., and Coleman, J.T.H. (2011). A five-year assessment of mortality
731 and geographic spread of white-nose syndrome in North American bats and a look to the future.
732 Bat Res. News *52*, 13–27.

733 Verant, M.L., Boyles, J.G., Waldrep, W., Wibbelt, G., and Blehert, D.S. (2012). Temperature-
734 dependent growth of *Geomyces destructans*, the fungus that causes bat white-nose syndrome.
735 Plos One *7*, e46280.

736 Verant, M.L., Meteyer, C.U., Speakman, J.R., Cryan, P.M., Lorch, J.M., and Blehert, D.S.
737 (2014). White-nose syndrome initiates a cascade of physiologic disturbances in the hibernating
738 bat host. BMC Physiol. *14*, 10.

739 Vonhof, M.J., Russell, A.L., and Miller-Butterworth, C.M. (2015). Range-wide genetic
740 analysis of little brown bat (Myotis lucifugus) populations: estimating the risk of spread of
741 White-nose syndrome. PLoS ONE *10*, e0128713.

742 Vonhof, M.J., Amelon, S.K., Currie, R.R., and McCracken, G.F. (2016). Genetic structure of
743 winter populations of the endangered Indiana bat (Myotis sodalis) prior to the white nose
744 syndrome epidemic: implications for the risk of disease spread. Conserv. Genet. *17*, 1025–
745 1040.

746 Voronin, D.A., and Kiseleva, E.V. (2007). [Functional role of proteins containing ankyrin
747 repeats]. Tsitologiia *49*, 989–999.

748 Warnecke, L., Turner, J.M., and Geiser, F. (2008). Torpor and basking in a small arid zone
749 marsupial. Naturwissenschaften *95*, 73–78.

750 Warnecke, L., Turner, J.M., Bollinger, T.K., Lorch, J.M., Misra, V., Cryan, P.M., Wibbelt, G.,
751 Blehert, D.S., and Willis, C.K.R. (2012). Inoculation of bats with European *Geomyces*
752 *destructans* supports the novel pathogen hypothesis for the origin of white-nose syndrome.
753 Proc. Natl. Acad. Sci. U. S. A. *109*, 6999–7003.

754 Warnecke, L., Turner, J.M., Bollinger, T.K., Misra, V., Cryan, P.M., Blehert, D.S., Wibbelt,
755 G., and Willis, C.K.R. (2013). Pathophysiology of white-nose syndrome in bats: a mechanistic
756 model linking wing damage to mortality. Biol. Lett. *9*, 20130177.

757 Wibbelt, G., Kurth, A., Hellmann, D., Weishaar, M., Barlow, A., Veith, M., Prueger, J.,
758 Goerfoel, T., Grosche, L., Bontadina, F., et al. (2010). White-nose syndrome fungus
759 (*Geomyces destructans*) in Bats, Europe. Emerg. Infect. Dis. *16*, 1237–1243.

760 Wibbelt, G., Puechmaille, S.J., Ohlendorf, B., Muehldorfer, K., Bosch, T., Goerfoel, T.,
761 Passior, K., Kurth, A., Lacremans, D., and Forget, F. (2013). Skin lesions in European
762 hibernating bats associated with *Geomyces destructans*, the etiologic agent of white-nose
763 syndrome. Plos One *8*, e74105.

764 Wilder, A.P., Kunz, T.H., and Sorenson, M.D. (2015). Population genetic structure of a
765 common host predicts the spread of white-nose syndrome, an emerging infectious disease in
766 bats. Mol. Ecol. *24*, 5495–5506.

767 Willis, C.K.R., Menzies, A.K., Boyles, J.G., and Wojciechowski, M.S. (2011). Evaporative
768 water loss is a plausible explanation for mortality of bats from white-nose syndrome. Integr.
769 Comp. Biol. *51*, 364–373.

770 Wright, S. (1978). Evolution and the Genetics of Populations, Volume 4. Variability within
771 and among Natural Populations. (Chicago: University of Chicago Press).

772 www.whitenosesyndrome.org (2019). White-nose syndrome occurance map - by year (2019).
773 Data last updated: 3/15/2019. Available at:
774 https://www.whitenosesyndrome.org/resources/map.

775 Yang, Z., Shi, H., Ma, P., Zhao, S., Kong, Q., Bian, T., Gong, C., Zhao, Q., Liu, Y., Qi, X., et
776 al. (2018). Darwinian Positive Selection on the Pleiotropic Effects of KITLG Explain Skin
777 Pigmentation and Winter Temperature Adaptation in Eurasians. Mol. Biol. Evol. 1–12.

778 Zeisset, I., and Beebee, T.J.C. (2014). Drift Rather than Selection Dominates MHC Class II
779 Allelic Diversity Patterns at the Biogeographical Range Scale in Natterjack Toads Bufo
780 calamita. PLOS ONE *9*, e100176.

781 Zhang, T., Victor, T.R., Rajkumar, S.S., Li, X., Okoniewski, J.C., Hicks, A.C., Davis, A.D.,
782 Broussard, K., LaDeau, S.L., Chaturvedi, S., et al. (2014). Mycobiome of the bat white nose
783 syndrome affected caves and mines reveals diversity of fungi and local adaptation by the fungal
784 pathogen *Pseudogymnoascus (Geomyces) destructans*. PLOS ONE *9*, e108714.

785 Zhang, T., Chaturvedi, V., and Chaturvedi, S. (2015). Novel *Trichoderma polysporum* strain
786 for the biocontrol of *Pseudogymnoascus destructans*, the fungal etiologic agent of bat white
787 nose syndrome. PLOS ONE *10*, e0141316.

788 Zukal, J., Bandouchova, H., Brichta, J., Cmokova, A., Jaron, K.S., Kolarik, M., Kovacova, V.,
789 Kubátová, A., Nováková, A., Orlov, O., et al. (2016). White-nose syndrome without borders:

790 *Pseudogymnoascus destructans* infection tolerated in Europe and Palearctic Asia but not in
791 North America. Sci. Rep. *6*, 19829.

792 **Table captions**

793 Table 1. Samples used in study. Pre-WNS-sites in grey circles and Post-WNS-sites in white
794 circles. 1) Aitkin Cave, Mifflin County, PA; 2) Snyder County, Penn, PA; 3) Lewisburg, Union
795 Co, PA; 4) Northumberland County, PA; 5) Howes Cave, County Schoharie, NY; 6)
796 Allentown, Lehigh County, PA; 7) Woodward, Centre County, PA; 8) Alexandria, Huntingdon
797 County, PA; 9) Lackawaxen, Pike County, PA; 10) Oley, County Berks, PA; 11) Frankstown,
798 County Blair, PA; 12) Williams Preserve Mine, NY; 13) Hoopers Mine, NY; 14) Delmar,
799 Albany County, NY; and 15) Willsboro, Essex County, NY.

800 Table 2. Summary of individual SNP F_{ST} values across the *M. lucifugus* genome when
801 comparing Pre-WNS with Post-WNS; and samples from PA and NY (both Pre- and Post-
802 WNS).

803 Table 3. Genes within the *M. lucifugus* genome – excluding scaffold GL429776 – with
804 windows possessing F_{ST} values >= 0.05 when comparing PA and NY samples Post-WNS

805 Table 4. Genes within scaffold GL429776 with windows possessing F_{ST} values >= 0.05 when
806 comparing PA and NY samples Post-WNS.

807 Figure captions

808 Fig. 1. *M. lucifugus* sampling locations in Pennsylvania (PA) and New York (NY). Sampling
809 sites sampled before the arrival of white-nose syndrome indicated with +, whereas sampling
810 locations for Post-WNS individuals (PA, NY) indicated with ●.

811 Fig. 2. Fixation indices (F_{ST}) across the *M. lucifugus* genome, comparing the population before
812 and after the arrival of white-nose syndrome. Scaffold lengths presented in green and blue.
813 Solid red line indicates cut-off for F_{ST} values of 5 standard deviations from the mean across
814 the whole genome; dotted red line indicates cut-off of F_{ST}=0.05.

815 Fig 3. Fixation indices (F_{ST}) across the *M. lucifugus* genome between geographically separated
816 individuals of the study population a) comparing individuals from PA to individuals from NY
817 before the arrival of WNS; b) comparing individuals from PA before and after the arrival of
818 WNS; and c) comparing individuals from NY before and after the arrival of WNS. Solid red
819 line indicates cut-off for F_{ST} values of 5 standard deviations from the mean across the whole
820 genome; dotted red line indicates cut-off of F_{ST}=0.05.

821 Fig 4. Fixation indices (F_{ST}) across the *M. lucifugus* genome between geographically separated
822 individuals of the study population a) comparing individuals from PA to individuals from NY
823 after the arrival of WNS, with a zoomed plot of scaffold GL429776 and gene models therein
824 containing windows demonstrating F_{ST} values < 0.05; and b) comparing individuals from PA
825 to individuals from NY with Pre- and Post-WNS data combined. Solid red line indicates cut-
826 off for F_{ST} values of 5 standard deviations from the mean across the whole genome; dotted red
827 line indicates cut-off of F_{ST}=0.05.

828 Fig 5. Proportions of reference alleles called at individual SNP sites for the region of scaffold
829 GL429776 demonstrating high F_{ST} values when comparing a) individuals from Pennsylvania
830 before and after the arrival of WNS; b) individuals from NY before and after the arrival of
831 WNS; c) individuals from PA to individuals from NY before the arrival of WNS; and d)
832 individuals from PA to individuals from NY after the arrival of WNS.

833 Table 1.

Sample age	Classification	Total number of samples	Pennsylvania*	New York*
2006	Pre-WNS	49	25	24
2007	Pre-WNS	3	3	
2015	Post-WNS	28	28	
2016	Post-WNS	139	82	57

* WNS first detected in New York in 2007 and PA in 2009

834

Table 2.

	Pre- vs post-WNS	**Between site (combining pre- and post-WNS)**
Median (Interquartile range)	0.0059 (0.0013 – 0.0171)	0.0057 (0.0013 – 0.0165)
Mean (s.d.)	0.0127 (0.0173)	0.0123 (0.0170)

Table 3.

Scaffold	Location range (bp)	Gene ID	Protein Function	Number of overlapping high F_{ST} windows
NW_005871715.1	288334 - 351644	102435296	bifunctional heparan sulfate N-deacetylase/N-sulfotransferase 4-like (partial)	4
NW_005871771.1	26662 - 48938	102441697	E3 ubiquitin-protein ligase TRIM7	1
NW_005871823.1	81353 - 213965	102428352	Ankyrin 2	7
NW_005871905.1	175 - 139344	102428043	calcium/calmodulin-dependent protein kinase type II subunit delta-like	10

NW_005872026.1	72042 - 101269	102443179	N-deacetylase and N-sulfotransferase 4 (partial)	1
NW_005872062.1	33266 - 86607	102428048	zinc finger GRF-type containing 1	1

Table 4.

Gene ID	F_{ST}	No of windows	No of windows	Start pos.	End pos.	Details

			(per 10kb)			
MGAT4C	0.0612	78	1.08	8999210	9724150	Glycosyltransferase that participates in the transfer of N-acetylglucosamine (GlcNAc) to the core mannose residues of N-linked glycans
CEP290	0.0679	12	1.01	10709418	10827912	Involved in early and late steps in cilia formation
ATP2B1	0.0826	12	0.89	12228178	12362389	The protein encoded by this gene belongs to the family of P-type primary ion transport ATPases characterised by the formation of an aspartyl phosphate intermediate during the reaction cycle. These enzymes remove bivalent calcium ions from eukaryotic cells against very large concentration gradients and play a critical role in intracellular calcium homeostasis.

KITLG	0.0706	10	1.13	11127130	11215731	Plays an essential role in the regulation of cell survival and proliferation, hematopoiesis, stem cell maintenance, gametogenesis, mast cell development, migration and function, and in melanogenesis.
POC1B	0.0686	7	0.74	12044678	12139811	Plays an important role in centriole assembly and/or stability and ciliogenesis
TMTC3	0.0872	6	1.00	10827719	10887502	Involved in the positive regulation of proteasomal protein degradation in the endoplasmic reticulum (ER), and the control of ER stress response.
GeneID:111824954	0.0693	5	1.14	11756928	11800690	uncharacterised LOC111824954
CUNH12orf50	0.0588	2	0.67	10663328	10693373	chromosome unknown C12orf50 homolog
GeneID:111824948	0.0816	2	1.13	11375011	11392720	uncharacterised LOC111824948

GeneID:111824949	0.0635	2	1.14	11802704	11820273	uncharacterised LOC111824949
CUNH12orf29	0.0488	1	0.71	10696290	10710421	chromosome unknown C12orf29 homolog
DUSP6	0.0603	1	2.26	11976039	11980455	Inactivates MAP kinases.
GeneID:111824955	0.0459	1	1.57	12101754	12108133	uncharacterised LOC111824955

Fig 1.

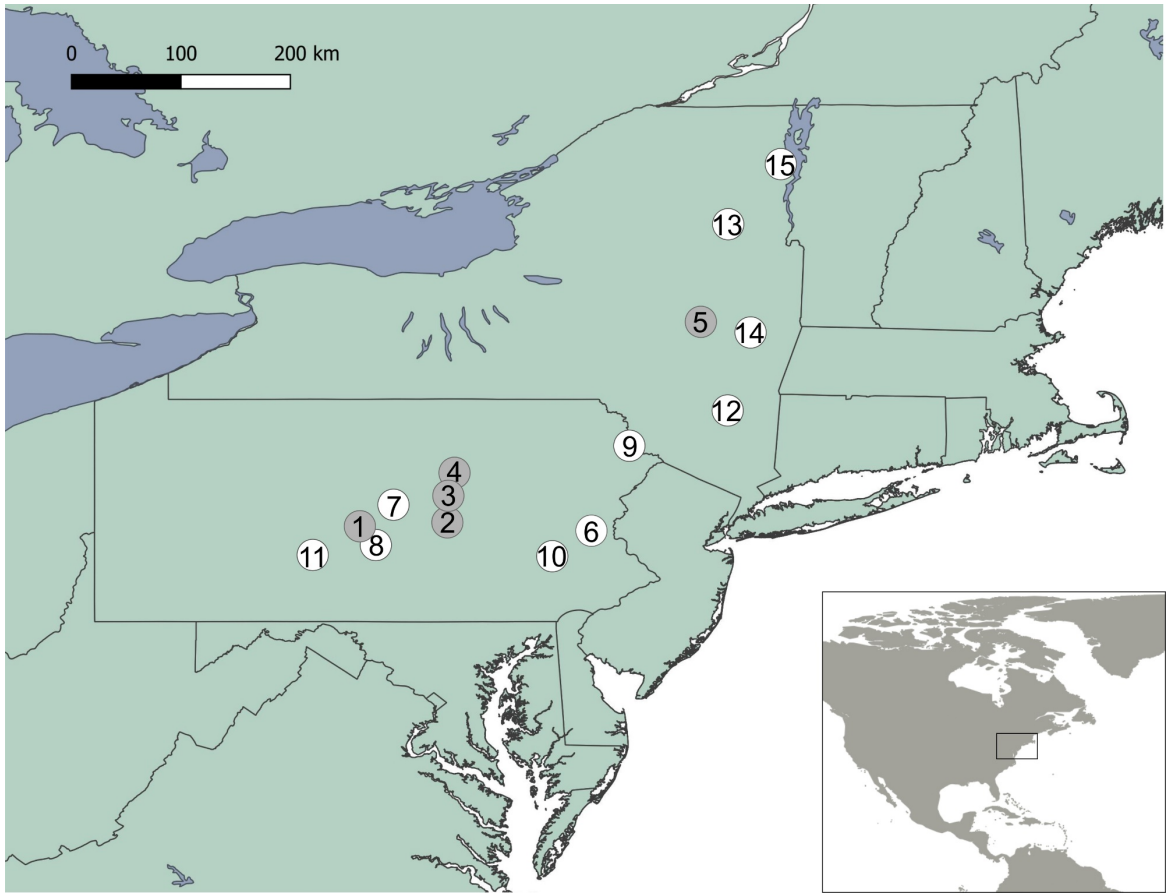

Fig. 2.

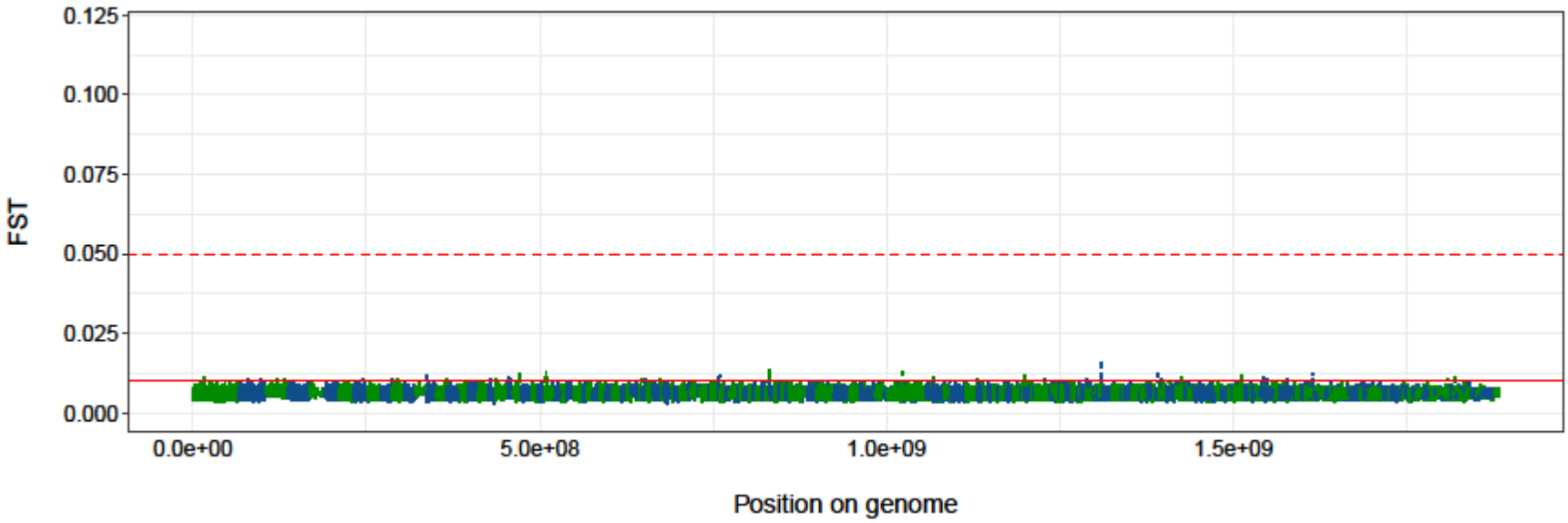
0.125
0.100
0.075
0.050
0.025
0.000
FST
0.0e+00
5.0e+08
1.0e+09
1.5e+09
Position on genome

Fig. 3.

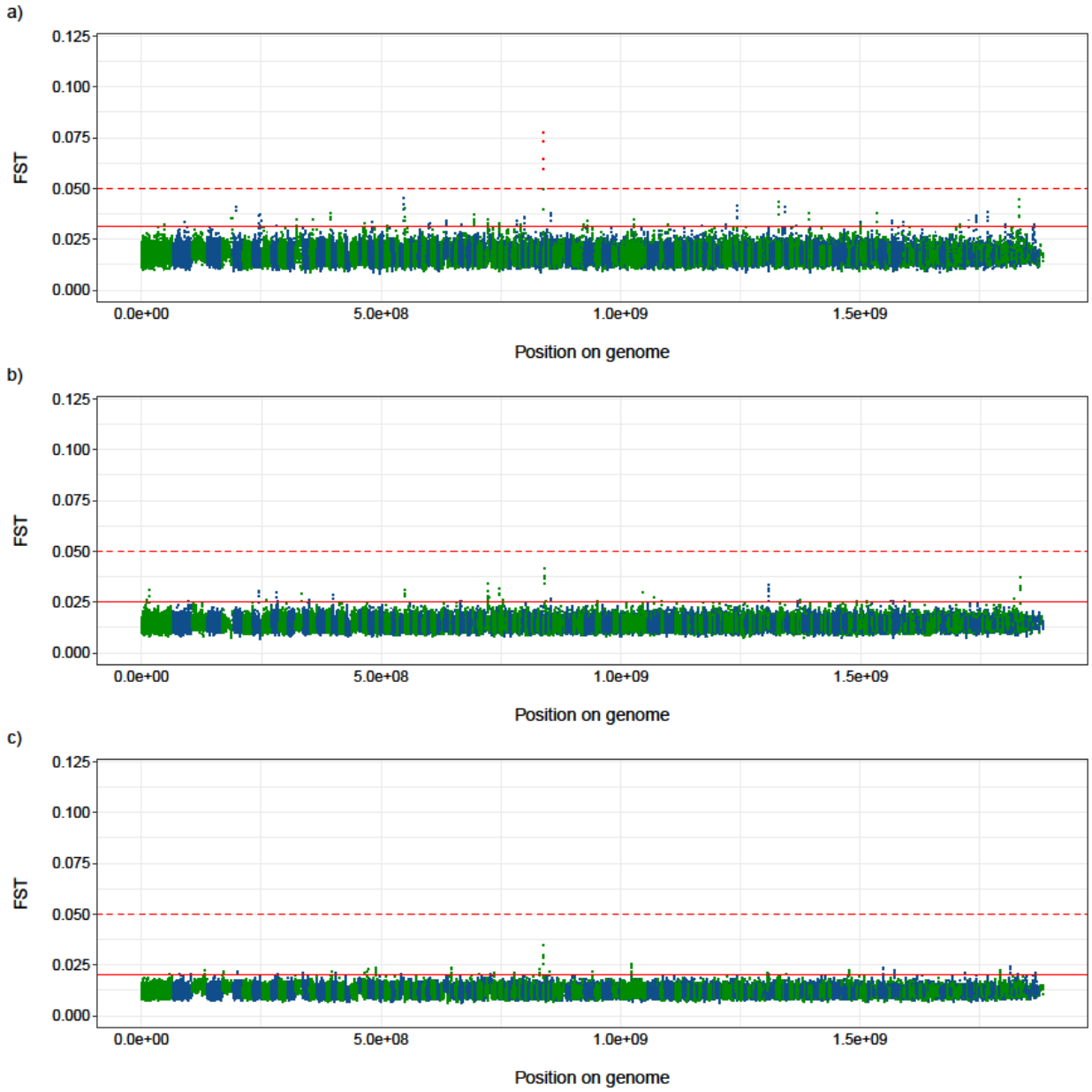
a)
FST
0.125
0.100
0.075
0.050
0.025
0.000
0.0e+00
5.0e+08
1.0e+09
1.5e+09
Position on genome
b)
FST
0.125
0.100
0.075
0.050
0.025
0.000
0.0e+00
5.0e+08
1.0e+09
1.5e+09
Position on genome
c)
FST
0.125
0.100
0.075
0.050
0.025
0.000
0.0e+00
5.0e+08
1.0e+09
1.5e+09
Position on genome

Fig 4.

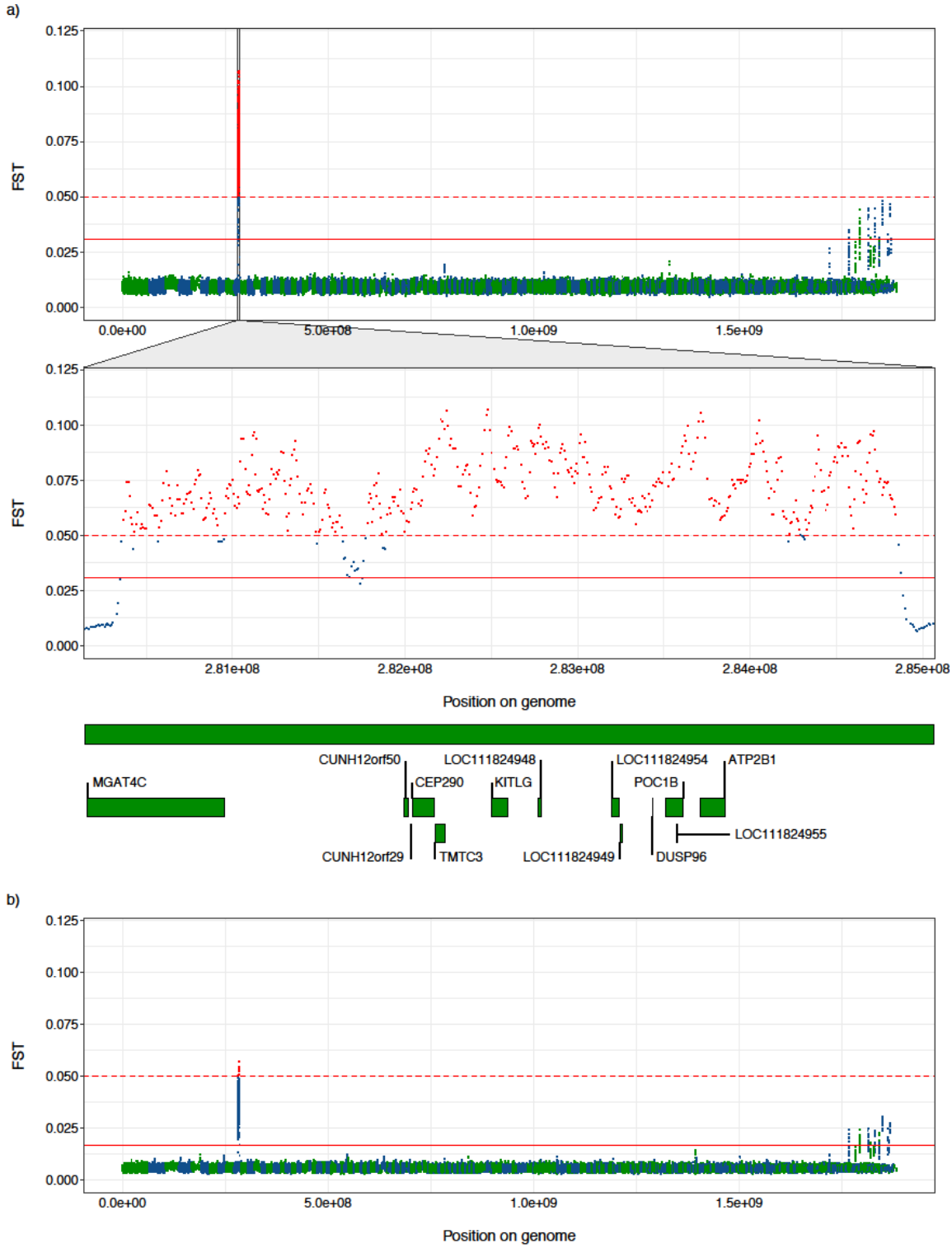
a)
FST
0.125
0.100
0.075
0.050
0.025
0.000
0.0e+00
5.0e+08
1.0e+09
1.5e+09
2.81e+08
2.82e+08
2.83e+08
2.84e+08
2.85e+08
Position on genome
MGAT4C
CUNH12orf50
CEP290
LOC111824948
KITLG
LOC111824954
POC1B
ATP2B1
LOC111824955
CUNH12orf29
TMTC3
LOC111824949
DUSP96
b)
FST
0.125
0.100
0.075
0.050
0.025
0.000
0.0e+00
5.0e+08
1.0e+09
1.5e+09
Position on genome

Fig 5.

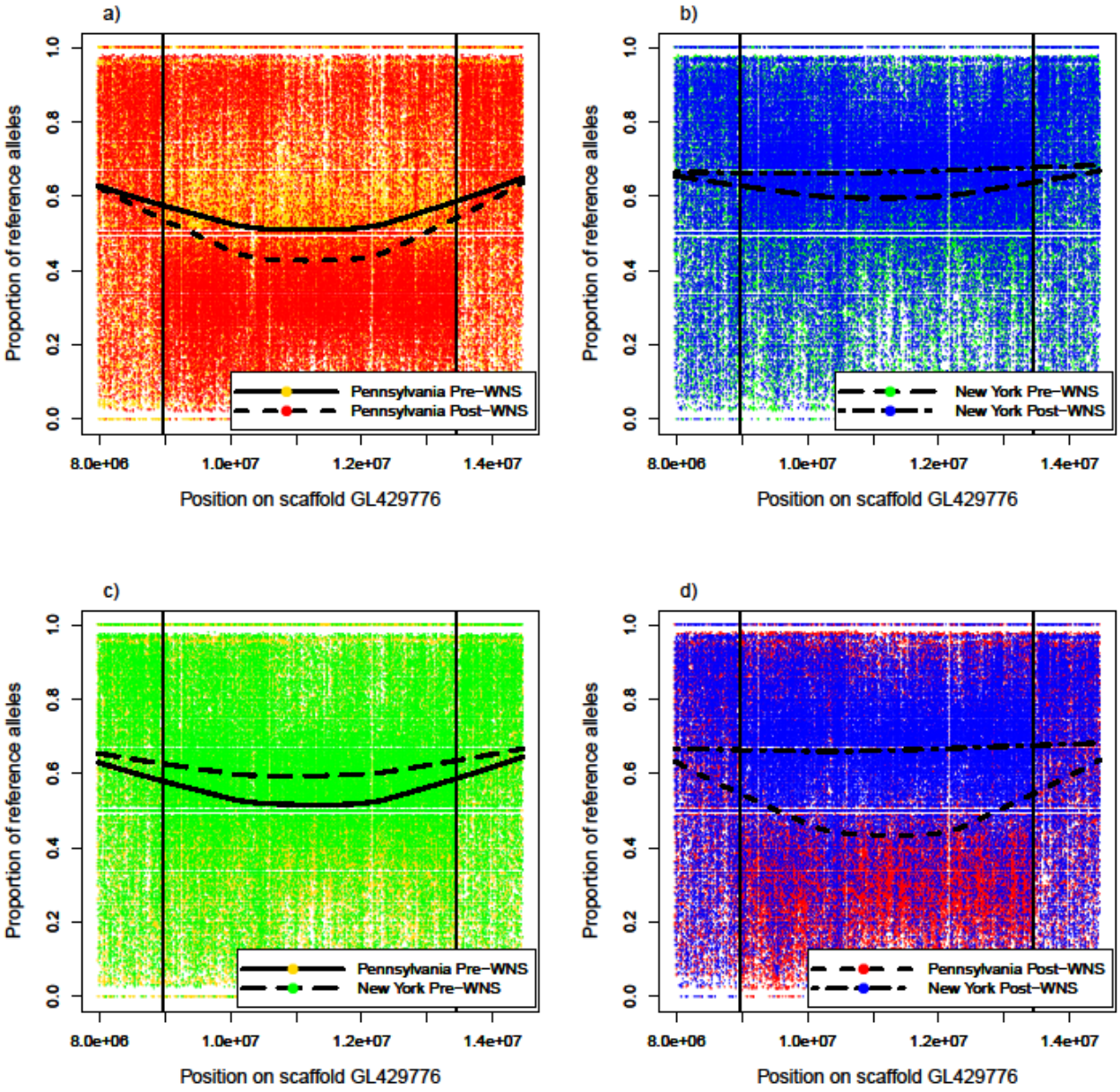
a)
b)
c)
d)
Proportion of reference alleles
0.0
0.2
0.4
0.6
0.8
1.0
8.0e+06
1.0e+07
1.2e+07
1.4e+07
Position on scaffold GL429776
Pennsylvania Pre–WNS
Pennsylvania Post–WNS
New York Pre–WNS
New York Post–WNS